

A novel fast numerical algorithm for cascaded Raman fiber laser using the analytic approximate solution

Huang Kaidi ^{a,*}, Zhou Xiaojun ^a, Qin Zujun ^a, Wu Haocheng ^b, Zhou Zili ^b

^a University of Electronic Science and Technology of China, School of Opto-electronic Information, Jianshe North Road, No. 4, Chengdu 610054, China

^b Guilin Institute of Optical Communications, Guilin 541004, China

Received 7 August 2006; received in revised form 12 October 2006; accepted 13 October 2006

Abstract

In this paper, we proposed a novel numerical algorithm for cascaded Raman fiber laser (CRFL) using the approximate analytic results as the initial values for shooting method, which effectively reduces the calculating time from several hours to a few minutes. With the algorithm, we obtained a numerical solution of the bilateral-pumping Ge-doped fifth-order CRFL which can avoid the so-called “end face damage” phenomenon efficiently. At the same time, we also simulated the unilateral-pumping one as a comparison, which showed both the characteristics of them are similar with each other.

© 2006 Elsevier B.V. All rights reserved.

Keywords: Cascaded fiber Raman laser; Numerical algorithm; Shooting; Bilateral pump

1. Introduction

The advents of the high-power pump laser source, the high Raman-gain fiber and the fiber Bragg grating (FBG) [1–5] make the realization of the all-fiber cascaded Raman fiber laser (CRFL) possible. With these devices, high-power pump light from a double-clad fiber laser is launched into a long low-loss and high Raman-gain silica-based fiber that are doped with either GeO₂ or P₂O₅ to exploit a potentially higher Raman gain or a wider frequency shift from the pump wavelength, respectively. With the application of FBGs designed to resonate the Stokes light, efficient down-shifted single-transverse-mode laser radiation is produced. Cascaded Raman fiber lasers are highly suitable for a number of direct and indirect applications such as the pumping of Raman fiber amplifiers and other fiber lasers.

CRFLs are generally described by a first-order system of nonlinear two-point boundary-value ordinary differential

equations (BVODEs) with the boundary conditions relating to the reflection coefficients of the mirrors at each end of the Raman fiber [6] which need shooting method in conjunction with Runge–Kutta method to solve numerically [7,8]. In the solution of BVODEs for an *n*th-order CRFL, there are *n* unknown parameters to be guessed as the initial values for the shooting method. The arbitrary initial values may make the converging procedure unstable and time-costing. On the other hand, the analytic method for design of CRFL has been developed recently [9], which have much faster speed with some approximation and assumption leading to error to the true. Taking the advantage of quickness of analytic method, we developed a novel numerical algorithm, adopting the analytic solution as the initial values of shooting method, which has the relatively high speed and accuracy.

Then, using the algorithm, we designed the bilateral-pumping fifth-order cascaded Ge-doped RFL, which has been seldom considered before. In the case of unilateral-pumping CRFL, as the input pump power increases to a relatively high level, the heat caused by the power at the input end can accumulate to such a high level that cause

* Corresponding author. Tel.: +86 13980598961; fax: +86 280131.

E-mail addresses: max_h1983@yahoo.com.cn (K. Huang), xjzhou@uestc.edu.cn (X. Zhou).

damage to the coating layer of fiber (end face damage). To avoid this problem bilateral pump can divide this high pump power into two parts, and inject them into the fiber at its both ends respectively.

2. Numerical model

As shown in Fig. 1, a fifth-order cascaded Raman fiber laser is composed of a silica-based Ge-doped fiber a few hundred meters in length and Bragg gratings placed at each end in order to resonate the intracavity Stokes fields.

The classical treatment of the steady-state Raman scattering processes resulting in fifth-order Stokes output from a cascaded Raman fiber laser is given by

$$\frac{1}{P_0^F(z)} \frac{dP_0^F(z)}{dz} = -\frac{1}{P_0^B(z)} \frac{dP_0^B(z)}{dz} = -\alpha_0 - \frac{\omega_0}{\omega_1} g_1 [P_1^F(z) + P_1^B(z)] \quad (1A)$$

$$\frac{1}{P_1^F(z)} \frac{dP_1^F(z)}{dz} = -\frac{1}{P_1^B(z)} \frac{dP_1^B(z)}{dz} = -\alpha_1 + g_0 [P_0^F(z) + P_0^B(z)] - \frac{\omega_1}{\omega_2} g_2 [P_2^F(z) + P_2^B(z)] \quad (1B)$$

$$\frac{1}{P_2^F(z)} \frac{dP_2^F(z)}{dz} = -\frac{1}{P_2^B(z)} \frac{dP_2^B(z)}{dz} = -\alpha_2 + g_2 [P_1^F(z) + P_1^B(z)] - \frac{\omega_2}{\omega_3} g_3 [P_3^F(z) + P_3^B(z)] \quad (1C)$$

$$\frac{1}{P_3^F(z)} \frac{dP_3^F(z)}{dz} = -\frac{1}{P_3^B(z)} \frac{dP_3^B(z)}{dz} = -\alpha_3 + g_3 [P_2^F(z) + P_2^B(z)] - \frac{\omega_3}{\omega_4} g_4 [P_4^F(z) + P_4^B(z)] \quad (1D)$$

$$\frac{1}{P_4^F(z)} \frac{dP_4^F(z)}{dz} = -\frac{1}{P_4^B(z)} \frac{dP_4^B(z)}{dz} = -\alpha_4 + g_4 [P_3^F(z) + P_3^B(z)] - \frac{\omega_4}{\omega_5} g_5 [P_5^F(z) + P_5^B(z)] \quad (1E)$$

$$\frac{1}{P_5^F(z)} \frac{dP_5^F(z)}{dz} = -\frac{1}{P_5^B(z)} \frac{dP_5^B(z)}{dz} = -\alpha_5 + g_5 [P_4^F(z) + P_4^B(z)]. \quad (1F)$$

The superscripts, “F” and “B”, in Eqs. (1A)–(1F) represent the forward- and backward-propagating pump (P_0) and the i th Stokes (P_i , in W) waves, respectively. Spontaneous Raman scattering has been neglected because that Raman oscillation is dominant, and it is assumed that all of the fields are unpolarized and that axial symmetry exists. The coefficients α_i are the values of the intrinsic loss of the host glass at the various field wavelengths, and ω_0 and ω_i are the frequencies of the pump and i th Stokes

waves respectively, and g_i is the experimentally determined Raman-gain coefficient. At the same time, the boundary conditions for the fifth-order cascaded Raman fiber laser at the input end of the fiber are given by

$$\begin{cases} P_0^F(0) = R_0^B P_0^B(0) + P_{in} \\ P_i^F(0) = R_i^B P_i^B(0) \end{cases} \quad \text{for } 1 \leq i \leq 5, \quad (2)$$

where the R_i^F is the reflectivity of the Bragg grating of the i th forward-propagating Stokes wave, which can be measured. In this model, we assumed the pump power deplete completely at the ends of the fiber, because the entire pump power is almost absorbed when the fiber length is longer than 100 m.

To solve Eq. (1) with the boundary conditions relating to the reflection coefficients of the FBGs at each end of the fiber, we note that the parameter $C_i = P_i^F P_i^B$ is a constant. Therefore, we introduce a new parameter θ_i , a dimensionless gain factor, to express the $P_i^{F/B}$ as follows:

$$\begin{cases} P_i^F = C_i \times \exp(\theta_i) \\ P_i^B = C_i \times \exp(-\theta_i). \end{cases} \quad (3)$$

So, the boundary conditions become

$$\begin{cases} \theta_0(0) = \ln(P_{in}/C_0), \\ \theta_i(0) = \ln(R_i^B)^{1/2}, \quad 1 \leq i \leq 5. \end{cases} \quad (4)$$

Additionally, in order to obtain a faster converging speed in shooting, we could get the value of the C_i , from the approximate analytic method [10] as the following:

$$\begin{cases} C_0 = P_0^F \times \exp(-(G'_1/G_1) \times P_0^F/2/(e_1 + (G_3/G'_3) \times (e_3 + e_5))) \\ C_1 = -\alpha_0/2/G_0 + (G'_1/G_1) \times P_0^F/2/(e_1 + (G_3/G'_3) \times (e_3 + e_5))/G_0/L \\ C_2 = (e_3 + e_5) \times (G_3/G'_3) \\ C_3 = (G'_2/G_2) \times (G'_1/G_1) \times P_0^F/2/(e_1 + C_2)/G_0/L \\ \quad - (e_2 + e_4) - (G'_2/G_2) \times \alpha_0/2/G_0 \\ C_4 = \alpha_5/2/G'_5 - \ln(R_5^F R_5^B)/4/G'_5/L \\ C_5 = C_3 \times (G'_4/G_4) \times \ln(R_5^F R_5^B)/2/A \end{cases} \quad (5)$$

where

$$G_i = g_{i+1} \times \frac{\omega_{i+1}}{\omega_i}, \quad 0 \leq i \leq 4$$

$$G'_i = g_i, \quad 0 \leq i \leq 5$$

$$e_i = \frac{\alpha_i}{2g_i} - \frac{\ln(R_i^F R_i^B)}{4g_i L}, \quad 0 \leq i \leq 5$$

$$A = \sinh(0.5 \times \ln(R_5^B)) + \sinh(0.5 \times \ln(R_5^F)).$$

With C_i , we can get the initial values from Eq. (3). Although there are still some errors between them and the modified initial values that satisfy the tolerance, which needs the “shooting” method to correct, the analytic initial values efficiently make an approach to the true value, which reduce the computing time considerably. To correct the input values, we set the target-output as

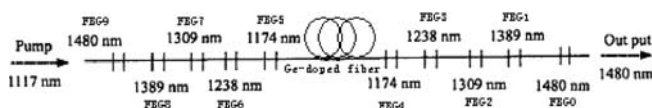


Fig. 1. Configuration of a fifth-order Ge-doped cascaded Raman fiber laser.

$$R_i^F = P_i^B(L)/P_i^F(L) \quad \text{for } 1 \leq i \leq 5, \quad (6)$$

where the R_i^F is the reflectivity of the Bragg grating of the i th forward-propagating Stokes wave.

Now the problem is to correct the input values that lead to corresponding outputs satisfying the boundary condition. We get the output matrix $Output(L)$ with its according input matrix $P(0)$. Then, we compare the $Output(L)$ with the target output matrix $Targetoutput(L)$ to decide whether the initial values satisfy the tolerance or not, and, if not, to modify the initial values. And these matrixes mentioned above are defined as follows:

$$\begin{aligned} Output(L) &= [P_1^B(L)/P_1^F(L), P_2^B(L)/P_2^F(L), P_3^B(L)/P_3^F(L), \\ &P_4^B(L)/P_4^F(L), P_5^B(L)/P_5^F(L)]^T \\ P(0) &= [P_1^B(0), P_2^B(0), P_3^B(0), P_4^B(0), P_5^B(0)]^T \\ Targetoutput(L) &= [R_1^F, R_2^F, R_3^F, R_4^F, R_5^F]^T. \end{aligned}$$

To modify these initial values, we need the assistance of the Jacobi matrix (J) in which its element is defined as Eq. (7).

$$\begin{aligned} J_{ij} &= \frac{\partial Error_i}{\partial P_j} \\ &= \frac{Error_i(P_0, \dots, (P_j + \Delta P_j), \dots) - Error_i(P_0, \dots, P_j, \dots)}{\Delta P_j}, \end{aligned} \quad (7)$$

where the matrix named $Error$ is defined as follows:

$$Error(L) = Output(L) - Targetoutput(L).$$

All in all, the main procedure is as follows. First we get the initial value $P(0)$ from approximate analytic method. Next, the coupled Eq. (1) is integrated by Runge–Kutta method, and the error between the $Output(L)$ and the $Targetoutput(L)$, $Error(L)$, is obtained. Then, the Jacobi matrix is calculated. Lastly the input is updated by adding $\Delta P(0) = J^{-1} \times Error(L)$. And the iteration will continue until the $Error(L)$ satisfies the error tolerance.

3. Results and discussion

With the algorithm mentioned above, we simulate both the unilateral-pumping cascaded Ge-doped RFL with pump power 10 W at input end, and the bilateral-pumping one with pump power 5 W at each ends. The reflectivity of

these FBGs is approximately 99% except the output coupler whose reflectivity is 16%. In both cases, the fiber length is 180 m, and its insert loss (L_i) at each FBG and splicing loss (L_s) at each splicing spot are 0.07 dB and 0.05 dB, respectively, and the Raman-gain and fiber attenuation coefficients are given by Table 1 and Table 2, respectively.

Taking account of the splicing and insert loss, we can get the efficient pump power and reflectivity, that is $P_0^{F'} = 10^{-0.5L_i - 0.6L_s} P_0^F$, $P_0^{B'} = 10^{-0.5L_i - 0.6L_s} P_0^B$, $R_1^{F'} = 10^{-0.8L_i - L_s} R_1^F$, $R_1^{B'} = 10^{-0.8L_i - L_s} R_1^B$, $R_2^{F'} = 10^{-0.6L_i - 0.8L_s} R_2^F$, $R_2^{B'} = 10^{-0.6L_i - 0.8L_s} R_2^B$, $R_3^{F'} = 10^{-0.4L_i - 0.6L_s} R_3^F$, $R_3^{B'} = 10^{-0.4L_i - 0.6L_s} R_3^B$, $R_4^{F'} = 10^{-0.2L_i - 0.4L_s} R_4^F$, $R_4^{B'} = 10^{-0.2L_i - 0.4L_s} R_4^B$, $R_5^{F'} = 10^{-0.2L_s} R_5^F$, $R_5^{B'} = 10^{-0.2L_s} R_5^B$. And our numerical simulation was done with less 1% tolerance for boundary conditions.

First of all, we did a comparison between the initial values given by the approximate analytic method and the ones modified by the ‘‘shooting’’ method to satisfy its tolerance, and the result is shown in Table 3. Obviously, there are still some errors between them, among which the maximum one is 7.35%. The reason is the analytic method is based on some approximations, which leads to relatively larger errors, and our numerical one without so many approximations, which results a better approach to the true value. With help of the initial value provided by the analytic method, the computing time is effectively shorten from several hours with arbitrary initial values to 3–5 min.

Up to now, the characteristics of the unilateral-pumping CRFL have been widely researched by many people, whilst the bilateral one has been never reached. For the first time, we simulated the bilateral-pumping CRFL, and the intracavity field power distributions of various waves are illustrated in Fig. 2.

From the figures we can see that the symmetric pump-power distribution makes the first–fourth Stokes waves

Table 3
Errors between the initial values

Factors	Initial values (W)	Modified values (W)	Errors (%)
P_1^B	2.3437	2.2767	2.94
P_2^B	1.0869	1.0836	0.22
P_3^B	1.9114	2.0339	6.02
P_4^B	0.9350	0.9308	0.45
P_5^B	1.8136	1.6893	7.35

Table 1
Raman-gain coefficients

g_1	g_2	g_3	g_4	g_5
4.72 (km W)^{-1}	4.31 (km W)^{-1}	3.95 (km W)^{-1}	3.53 (km W)^{-1}	3.03 (km W)^{-1}

Table 2
Fiber attenuation coefficients

α_0	α_1	α_2	α_3	α_4	α_5
2.12 (dB/km)	1.75 (dB/km)	1.54 (dB/km)	1.17 (dB/km)	2.63 (dB/km)	0.76 (dB/km)

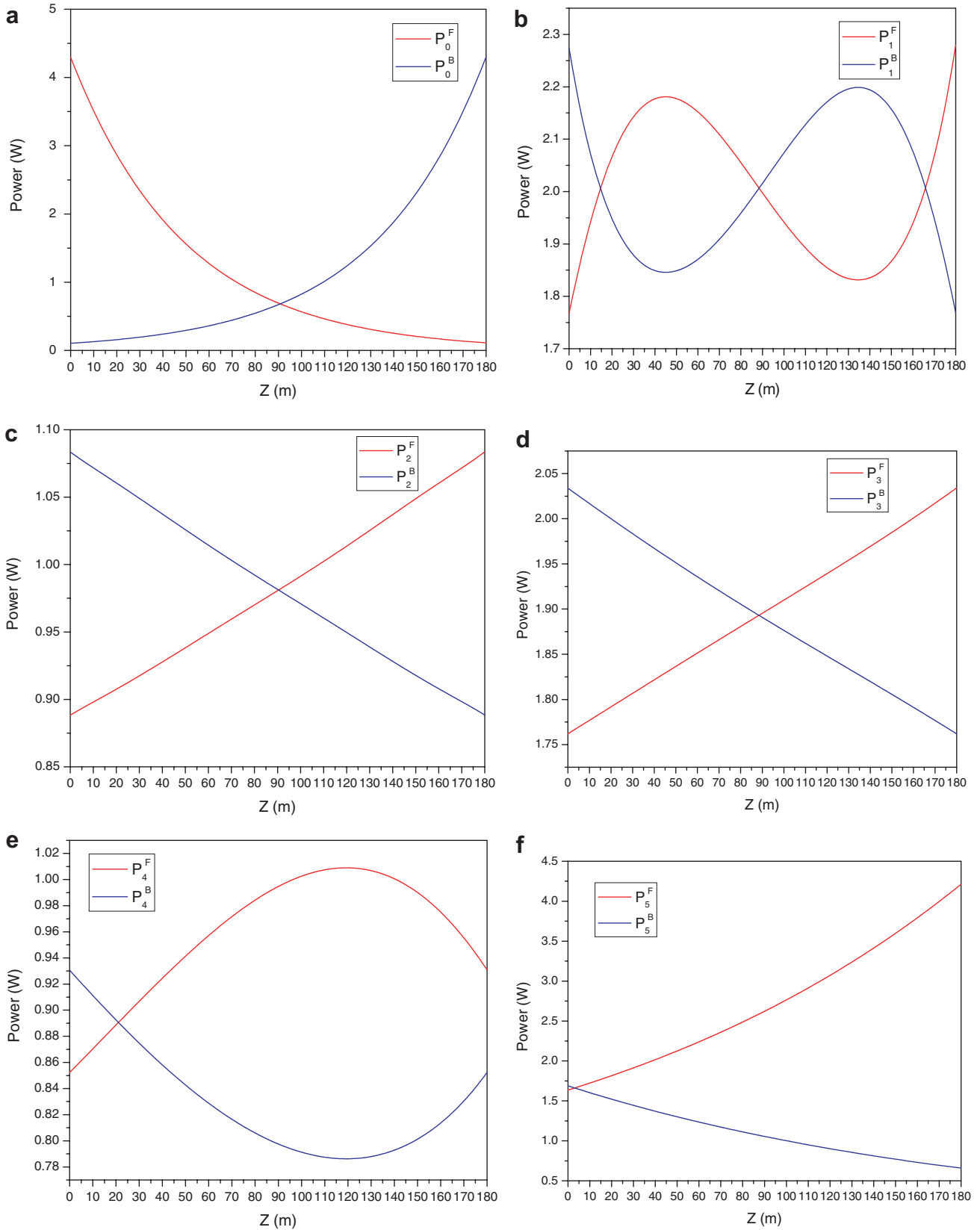


Fig. 2. Pump power and lasing power evolution along the fiber: (a) pump wave, (b) first Stokes wave, (c) second Stokes wave, (d) third Stokes wave, (e) fourth Stokes wave, (f) fifth Stokes wave.

have a good symmetry. Its output power and conversion efficiency is about 3.55 W and 35.5%, respectively, which is very close to the one of the unilateral-pumping fifth-order cascaded Ge-doped RFL (36.4%) in the same condition.

Besides, in Fig. 3 we also got the relationship between the input pump and the output lasing power, and made a comparison between the bilateral-pumping one and the unilateral-pumping one. It can be seen that there is almost linear relationship between the input pump power and the output power. And the threshold pump power is about 3.6 W. And its slope efficiency is about 55%, which is a little smaller than the one (56%) of the unilateral-pumping one.

Additionally, we also have shown the relationship between the reflectivity coefficient at the lasing wavelength at the output end and the output power in Fig. 4. The pump power is fixed to be 10 W (5 W at each ends). It can be seen that the laser reaches the maximum output when the reflectivity is around 15%. Here we also calculated the unilateral-pumping one as a comparison.

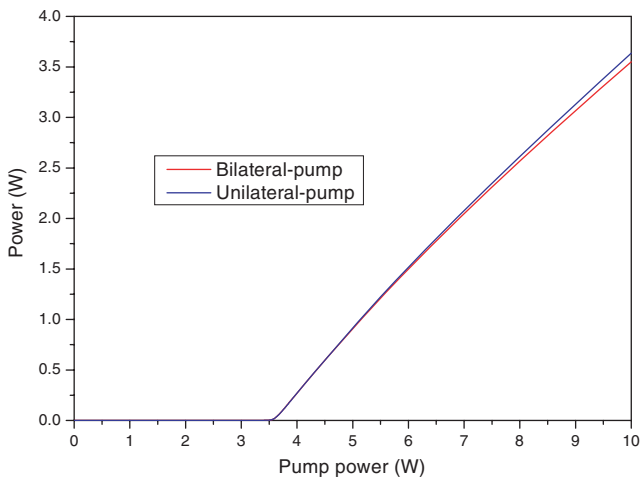


Fig. 3. The output power versus input pump power.

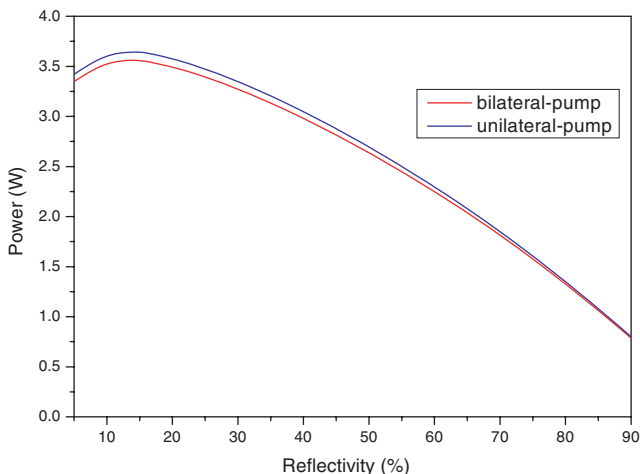


Fig. 4. The output power versus reflectivity at output end.

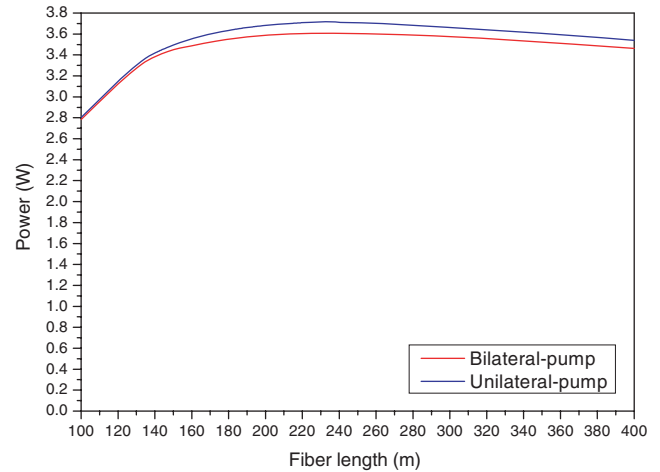


Fig. 5. The output power versus fiber length.

Besides, we illustrated the relationship between the fiber length and the output power in Fig. 5 in both cases of unilateral pump and the bilateral pump. In both cases, it can be seen that the laser reaches the maximum output when the fiber length is around 250 m, but the unilateral-pumping one is 3% high than the bilateral-pumping one. The reason is that the pump power in bilateral-pumping one suffered more insert losses and splicing losses before it reaches the Raman-gain medium. Additionally, we also can find the output power decrease gradually as the fiber length becomes longer.

Similarly, we did some research on the bilateral pumped fifth-order cascaded Ge-doped RFL with asymmetric pump power input either, and we found that there is no big difference between the asymmetric and the symmetric.

4. Conclusion

We proposed a new algorithm which has a quick converging speed and good stability because the analytic results are used as initial value in the “shooting” method. In our calculation, this algorithm effectively reduces the shooting time from several hours with arbitrary initial values to just a few minutes. Using this algorithm, we simulated the bilateral-pumping cascaded Ge-doped RFL and the unilateral-pumping one. Although, these characteristics of bilateral-pumping RFL are similar with the unilateral-pumping one, it is an effective way to avoid the “end face damage” phenomenon, which can fortify its stability and prolong its life-span. Additionally, we also did some optimization of this cascaded Raman fiber laser under certain level of pump power to maximize the energy conversion efficiency.

References

- [1] P. Persephonis, S.V. Chernikov, J.R. Taylor, *Electron. Lett.* 32 (1996) 1486.
- [2] E.M. Dianov, M.V. Grekov, I.A. Bufetov, S.A. Vasiliev, O.I. Medvedkov, V.G. Plotnichenko, V.V. Koltashev, A.V. Belov, M.M.

- Bubnov, S.L. Semjonov, A.M. Prokhorov, *Electron. Lett.* 33 (1997) 1542.
- [3] V.I. Karpov, E.M. Dianov, V.M. Paramonov, O.I. Medvedkov, M.M. Bubnov, S.L. Semjonov, S.A. Vasiliev, V.N. Protopopov, O.N. Egorova, V.F. Hopin, A.N. Guryanov, M.P. Bachynski, W.R.L. Clements, *Opt. Lett.* 24 (1999) 887.
- [4] N.S. Kim, M. Prabhu, C. Li, J. Song, K. Ueda, *Opt. Commun.* 176 (2000) 219.
- [5] E.M. Dianov, I.A. Bufetov, M.M. Bubnov, M.V. Grekov, S.A. Vasiliev, O.I. Medvedkov, *Opt. Lett.* 25 (2000) 402.
- [6] J. Auyeung, A. Yariv, *IEEE J. Quantum Electron.* QE-14 (1978) 347.
- [7] F. Leplingard, C. Martinelli, S. Borne, L. Lorcy, D. Bayart, F. Castella, P. Chartier, E. Faou, *IEEE Photon. Technol. Lett.* 16 (2004) 2601.
- [8] J.H. Zhou, J.P. Chen, X.W. Li, G.L. Wu, W.N. Jiang, C.H. Shi, Y.P. Wang, *Optics Express* 14 (2006) 3427.
- [9] B. Burgoyne, N. Godbout, S. Lacroix, *J. Opt. Soc. Am.* 22 (2005) 764.
- [10] Z.J. Qin, X.J. Zhou, Q. Li, An improved analytical approach for n th-order cascaded Raman fiber laser, in preparation.